PERGAMON

International Journal of Heat and Mass Transfer 44 (2001) 1465–1474

International Journal of HEAT and MASS TRANSFER

www.elsevier.com/locate/ijhmt

Forced convective boiling of binary mixtures in annular flow. Part I: liquid phase mass transport

J.R. Barbosa Jr., G.F. Hewitt *

Department of Chemical Engineering and Chemical Technology, Imperial College of Science, Technology and Medicine, London SW7 2BY, UK

Received 5 November 1999; received in revised form 20 June 2000

Abstract

This is the first part of a paper devoted to the description of forced convective boiling of binary mixtures at high qualities. Here, a model for droplet interchange (entrainment and deposition) in the annular flow regime in vertical pipes is presented. This is based on the set of correlations proposed by Govan et al. (A.H. Govan, G.F. Hewitt, D.G. Owen, T.R. Bott, in: Proceedings of the Second UK National Heat Transfer Conference, Institution of Mechanical Engineers, London, UK, 1988, p. 33) for pure fluids. It is shown that interaction of droplet entrainment, deposition and transport give rise to a local discrepancy between mean concentrations of the liquid film and entrained droplets. Also, the results reveal the importance of the initial entrained fraction (amount of liquid entrained as droplets at the onset of annular flow); variation of this parameter influences the downstream distributions of concentration in both liquid streams. The detailed analysis for heat and mass transfer is discussed in the second part of the paper.

1. Introduction

Phase change heat transfer to mixtures is of indisputable importance to the chemical and process industries. For instance, by definition, feeds to distillation tower reboilers are mixtures of two or more substances. In some cases, as in a typical petroleum feed, up to 40 pure substances may form the mixture. Despite the evident relevance of the subject, there is a dearth of experimental data and of adequately predictive methods for boiling of hydrocarbon mixtures.

Experimental data obtained recently using a high pressure multicomponent boiling rig at the Harwell laboratory of AEA Technology revealed many new features of forced convective multicomponent evaporation [2,3]. For instance, the increase in the heat transfer coefficient with quality characteristic of forced convective boiling often did not occur in these systems; indeed the coefficient sometimes actually decreases with increasing quality. These trends are not predicted either quantitatively or qualitatively by existing methods and was this failure in prediction which led to the present work. Kandlbinder et al. [2,3] suggest that these trends may be due to the development of differences in liquid composition of the drops and liquid film.

The objective of this two-part paper is to present a comprehensive model for flow and heat transfer of a binary mixture undergoing phase change in a vertical pipe. The model is for high mass qualities (annular flow regime), where nucleate boiling is expected to be greatly suppressed by forced convective mechanisms. In Part I, a model for droplet interchange, based on the set of correlations by Govan et al. [1] for pure fluids, is presented and embedded into a model for solving the hydrodynamics of the annular flow regime. Part II deals with heat and mass transfer. An important function of the analysis described in Part I of this paper is that it allows groups of droplets entrained at one location in the channel to be tracked downstream so that the number of these droplets remaining at any given downstream location can be determined; clearly, deposition of a proportion of this group of droplets will cause a reduction of the number

* Corresponding author.

0017-9310/01/$ - see front matter
PII: S0017-9310(00)00209-X

Nomenclature

C	concentration of droplets in the core, kg m^{-3}
d_p	diameter of a droplet, m
d_T	diameter of tube, m
D	deposition rate, kg m^{-2} s^{-1}
e	mass fraction defined in Eq. (36)
f	friction factor
F	function in system of Eq. (18), m s^{-2}
E	entrainment rate, kg m^{-2} s^{-1}
g	acceleration of gravity, m s^{-2}
k_D	deposition rate coefficient, m s^{-1}
$\dot{m}$	mass flux, kg m^{-2} s^{-1}
M_p	mass of a single droplet, kg
n	flux of droplets per unit area of tube wall, m^{-2} s^{-1}
NOD	flux of droplets per unit tube cross-sectional area, m^{-2} s^{-1}
p	pressure, Pa
$\dot{q}$	heat flux, W m^{-2}
Re	Reynolds number
u	velocity, m s^{-1}
u_{GS}	superficial velocity of gas, m s^{-1}
We	Weber number
x	composition of liquid (mass fraction)
y	composition of vapour (mass fraction)
z	axial co-ordinate, m

Greek symbols

δ	liquid film thickness, m
η	viscosity, N s m^{-2}
ρ	density, kg m^{-3}
σ	surface tension, N m^{-1}
τ	shear stress, N m^{-2}
Ψ	parameter defined in Eq. (20), m^3
Ω	parameter defined in Eq. (19), m s^{-1}

Subscripts

a	accelerational
c	creation
C	core
D	deposition
E	entrainment
f	frictional
g	gravitational
GC	gas core
i	component identifier, 1-pentane
I	interface
LE	entrained liquid
LF	liquid film
LFC	critical liquid film
OA	onset of annular flow
T	total
w	wall

Superscripts

j, k, m	axial co-ordinate (section) counters

with axial distance. A group of droplets generated at a given location is assumed to have a composition (i.e., mole fractions of each component) which is identical to the mean composition of the liquid film at that location, the group of droplets being entrained from this film. Thus, the average composition of the droplets at any axial position will depend on the distribution of origins of the droplets and on the film composition at these origins. At this axial position, therefore, the average composition in the entrained drop and film flows may be very different. In Part I illustrative calculations are given, which rely on calculation of film composition which are described in Part II. These calculations illustrate the fact that large differences in film and average drop compositions can develop, confirming the hypothesis of Kandlbinder et al. [2,3]. The effects of these composition differences in heat and mass transfer are explored in Part II of this paper. In Part I, we are primarily concerned with the modelling of the *hydrodynamics* of the annular flow to form a basis for the heat and mass transfer analysis in Part II.

The mass interchange process between the liquid film (continuous) and entrained (dispersed droplet) streams is at the kernel of annular flow modelling. The influence it exerts on the behaviour of some important flow properties is very high and, in order to improve the accuracy of the predictions of such parameters, several correlations for entrainment and deposition rates were suggested over the past years [1,4–6]. In flows where thermodynamic non-equilibrium prevails, closure is obtained via the adoption of additional hypotheses so as to specify spectra of droplet sizes and/or velocities. Whalley et al. [7] incorporated correlations for such parameters and reported a very good agreement between prediction and experimental data for the cases of post dryout heat transfer and condensation of superheated vapours. In the present work, a similar methodology was implemented for the calculation of droplet sizes.

In what follows, Section 2 presents a detailed description of the modelling framework, including the proposed droplet interchange model. The results are shown in Section 3. Axial distributions of pressure and of mean concentration (mass fraction) in both film and droplet streams are presented for various conditions. The behaviour of the mean concentration of the liquid film and droplets is highly influenced by the amount of liquid entrained as droplets at the onset of annular flow. Finally, conclusions are drawn in Section 4.

2. Modelling

2.1. Entrainment and deposition

The present representation of the physics of the problem is schematically illustrated in Fig. 1. The portion of the vertical pipe over which annular flow occurs is divided into M sections, 0 being the section at which the onset of annular flow takes place. The initial bulk concentrations (in terms of mass fractions) of the ith component in the liquid film, entrained droplets and vapour core are $x^0_{\mathrm{LF},i}$, $x^0_{\mathrm{LE},i}$ and $y^0_{\mathrm{GC},i}$, respectively. An initial value is assumed for the fraction of liquid entrained as droplets at the point of initiation of the annular regime $(m = 0)$ and the concentration of the respective components in this initially entrained liquid is assumed equal (at this point) to that of the liquid film – though differences develop later. The transition to annular flow is determined by the critical velocity criterion for flow reversal by Wallis [8]

$$u^*_{\mathrm{GS}} = 1.0, \tag{1}$$

where

$$u^*_{\mathrm{GS}} = u_{\mathrm{GS}}\sqrt{\frac{\rho_{\mathrm{G}}}{gd_{\mathrm{T}}(\rho_{\mathrm{L}} - \rho_{\mathrm{G}})}}. \tag{2}$$

The number per unit time per unit area of tube wall of droplets that deposit at section m is defined as

$$\langle n^m_{\mathrm{D}}\rangle = \sum_{j=0}^{m} n^{j,m}_{\mathrm{D}}, \tag{3}$$

where $n^{j,m}_{\mathrm{D}}$ is the number per unit time per unit area of tube wall of droplets entrained at section j (lower than m) that deposit at section m. Analogously, n^m_{E} is defined as the number per unit time per unit area of tube wall of droplets created (entrained) at section m. If the entrainment and deposition rates at any point in the channel are known, $n^{j,m}_{\mathrm{D}}$ and n^m_{E} are given by Bennett et al. [9]

$$n^m_{\mathrm{E}} = \frac{E^m}{M^m_{\mathrm{pc}}}, \tag{4}$$

and

$$n^{j,m}_{\mathrm{D}} = \frac{D^{j,m}}{M^{j,m}_{\mathrm{p}}}, \tag{5}$$

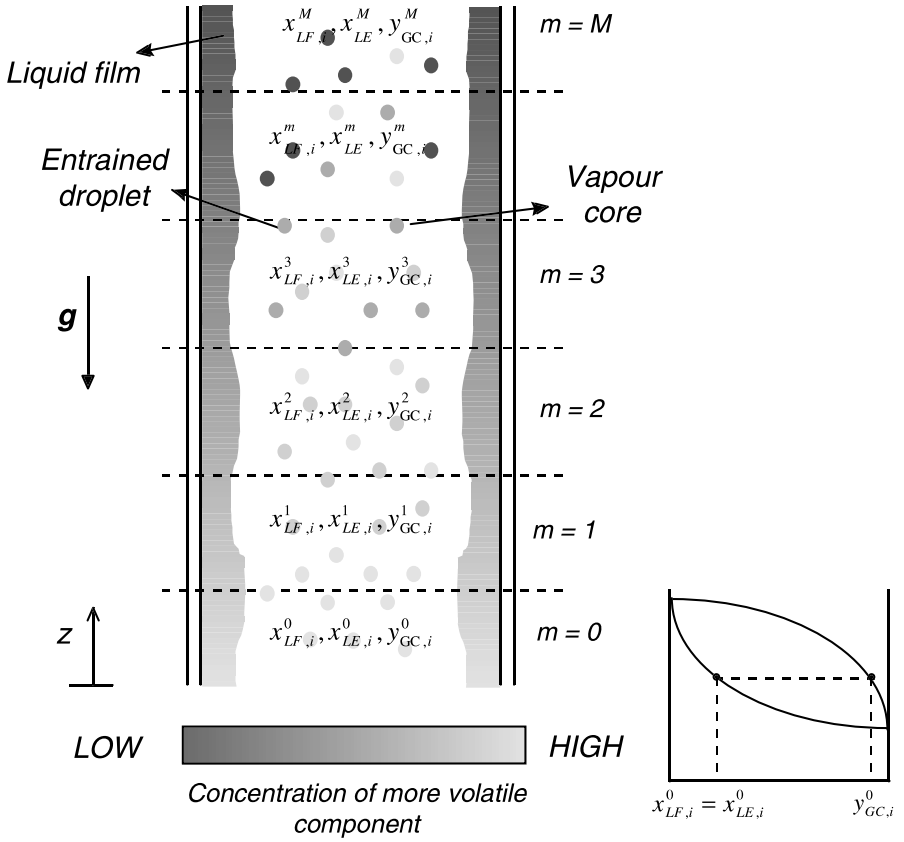

Fig. 1. Illustration of the problem.

where M_{pc}^{m} and $M_{p}^{j,m}$ are the mass of a droplet at creation at a section m and the mass, at section m, of a droplet generated at section j, respectively. If droplet evaporation and break-up/coalescence effects are not considered, then $M_{p}^{j,m} = M_{pc}^{m}$. Assuming that the droplets have a spherical shape, M_{pc}^{m}, is given by

$$M_{pc}^{m} = \frac{\pi \rho_{LF}^{m} (d_{pc}^{m})^{3}}{6}, \tag{6}$$

where d_{pc}^{m} is the diameter of a droplet when created at section m. In the present work, d_{pc} is calculated through a correlation by Azzopardi et al. [10] for the Sauter mean diameter of droplets in vertical annular flow. This is as follows:

$$\frac{d_{pc}}{d_T} = 1.91 \frac{Re_G^{0.1}}{We^{0.6}} + 0.4 \frac{\dot{m}_{LE}}{\rho_L u_{GS}}, \tag{7}$$

where the Weber number and the gas phase Reynolds numbers are given by

$$We = \frac{\rho_G u_{GS}^2 d_T}{\sigma}, \tag{8}$$

and

$$Re_G = \frac{\rho_G u_{GS} d_T}{\eta_G}. \tag{9}$$

The second term in the RHS of Eq. (7) accounts for coalescence and was not used in the present analysis since such coalescence is likely to be small. The entrainment and deposition rates, E^{m} and $D^{j,m}$, are a modification to the set of correlations developed by Govan et al. [1]. These are as follows:

$$E^{m} = \begin{cases} 0 \quad \text{if } \dot{m}_{LF}^{m} \leqslant \dot{m}_{LFC}^{m}, \\ 5.75 \times 10^{-5} \dot{m}_{GC}^{m} \left[\frac{\rho_{LF}^{m} d_T}{\sigma_{LF}^{m} \rho_G^2} (\dot{m}_{LF}^{m} - \dot{m}_{LFC}^{m})^2 \right]^{0.316} \\ \quad \text{if } \dot{m}_{LF}^{m} > \dot{m}_{LFC}^{m}, \end{cases} \tag{10}$$

where $\dot{m}_{LFC}^{m}$ is a critical liquid film mass flux given by

$$\dot{m}_{LFC}^{m} = \frac{\eta_{LF}^{m}}{d_T} \exp \left[5.8504 + 0.4249 \left(\frac{\eta_G^{m}}{\eta_{LF}^{m}} \right) \left(\frac{\rho_{LF}^{m}}{\rho_G} \right)^{0.5} \right]. \tag{11}$$

The droplet deposition rate is expressed as:

$$D^{j,m} = k_D^{j,m} C^{j,m}, \tag{12}$$

where $C^{j,m}$ is the concentration, at section m, of droplets entrained at section j

$$C^{j,m} = \frac{\dot{m}_{LE}^{j,m}}{(\dot{m}_G^{m}/\rho_G^{m}) + \langle \dot{m}_{LE}^{m}/\rho_{LE}^{m} \rangle}, \tag{13}$$

and the deposition transfer coefficient, $k_D^{j,m}$, is given by

$$k_D^{j,m} = \begin{cases} 0.18 \left(\frac{\sigma_{LE}^{j,m}}{\rho_G^{m} d_T} \right)^{0.5} & \text{if } \frac{\langle C^{m} \rangle}{\rho_G^{m}} \leqslant 0.3, \\ 0.18 \left(\frac{\rho_G^{m}}{\langle C^{m} \rangle} \right)^{0.65} \left(\frac{\sigma_{LE}^{j,m}}{\rho_G^{m} d_T} \right)^{0.5} & \text{if } \frac{\langle C^{m} \rangle}{\rho_G^{m}} > 0.3. \end{cases} \tag{14}$$

$\langle C^{m} \rangle$ is the cumulative droplet concentration defined as

$$\langle C^{m} \rangle = \frac{\langle \dot{m}_{LE}^{m} \rangle}{(\dot{m}_G^{m}/\rho_G^{m}) + \langle \dot{m}_{LE}^{m}/\rho_{LE}^{m} \rangle} \tag{15}$$

with the cumulative operator $\langle\,\rangle$ defined in Eq. (3).

The number flowing per unit time per unit pipe cross-sectional area, at section m, of droplets generated at section j, $NOD^{j,m}$, can be calculated through a balance in the vapour core over a length Δz. This gives

$$\frac{\Delta NOD^{j,m}}{\Delta z} = \frac{4}{d_T} \left(n_E^{j} - \sum_{k=j}^{m} n_D^{j,m} \right). \tag{16}$$

Writing $NOD^{j,m}$ in terms of $\dot{m}_{LE}^{j,m}$,

$$NOD^{j,m} = \frac{\dot{m}_{LE}^{j,m}}{M_p^{j,m}}. \tag{17}$$

After some algebraic manipulation, a combination of Eqs. (4)–(17) leads to the following system of equations:

$$F^{j,m} \equiv \Omega^{j,m} \left(n_E^{j} - \sum_{k=j}^{m} n_D^{j,k} \right) - n_D^{j,m} \left[\frac{\dot{m}_{GC}^{m}}{\rho_G^{m}} + \sum_{j=0}^{m} \Psi^{j,m} \left(n_E^{j} - \sum_{k=j}^{m} n_D^{j,k} \right) \right] = 0, \tag{18}$$

where

$$\Omega^{j,m} = \frac{4 \Delta z}{d_T} k_D^{j,m}, \tag{19}$$

and

$$\Psi^{j,m} = \frac{4 \Delta z}{d_T} \frac{M_p^{j,m}}{\rho_{LE}^{j,m}}. \tag{20}$$

The above $(m+1) \times (m+1)$ system of equations is solved for $n_D^{j,m}$ via a multi-dimensional Newton–Raphson algorithm [11]. The elements of the associated Jacobian matrix, $(\partial F^{j,m}/\partial n_D^{j,m})$, are given by

$$\frac{\partial F^{j,m}}{\partial n_D^{j,m}} = \begin{cases} -\Omega^{j,m} - \left[\frac{\dot{m}_{GC}^{m}}{\rho_G^{m}} + \sum_{j=0}^{m} \Psi^{j,m} \left(n_E^{j} - \sum_{k=j}^{m} n_D^{j,k} \right) \right] \\ \quad + \Psi^{j,m} n_D^{j,m} \quad \text{if } j = k, \\ \Psi^{k,m} n_D^{j,m} \quad \text{if } j \neq k. \end{cases} \tag{21}$$

Due to the non-linearity involving $\langle C^{m} \rangle$ and $k_D^{j,m}$ in the second portion of Eq. (14), the Newton–Raphson algorithm was implemented as a part of an outer, self-converging, iterative scheme. The initial condition for $n_D^{j,m}$ was set equal to $0.001 n_E^{j}$.

2.2. The annular flow model

The calculation framework described in Section 2.1 was embodied into an annular flow modelling programme (GRAMP code, [12]) in which the triangular relationship between film thickness, film flow rate and interfacial shear stress is invoked together with the relationships for entrainment and deposition rates. In its simplest form, the triangular relationship can be expressed as:

$$\dot{m}_{\mathrm{LF}} = \frac{4}{d_{\mathrm{T}}}\delta\sqrt{\frac{2\tau_{\mathrm{I}}\rho_{\mathrm{LF}}}{f_{\mathrm{LF}}}}, \tag{22}$$

where f_{LF} is the liquid film friction factor. f_{LF} is derived from results for the integration of the turbulent velocity profile in the liquid film [13] expressed in non-dimensional form as friction factor as a function of film Reynolds number [14], this function being fitted numerically. The interfacial shear stress is given by

$$\tau_{\mathrm{I}} = \frac{1}{2}\rho_{\mathrm{C}} f_{\mathrm{I}}(u_{\mathrm{C}} - u_{\mathrm{I}})^2, \tag{23}$$

where ρ_{C} and u_{C} are the homogeneous core density and mean velocity. These are given by

$$\rho_{\mathrm{C}} = \frac{\dot{m}_{\mathrm{LE}} + \dot{m}_{\mathrm{GC}}}{(\dot{m}_{\mathrm{LE}}/\rho_{\mathrm{LE}}) + (\dot{m}_{\mathrm{GC}}/\rho_{\mathrm{GC}})}, \tag{24}$$

and

$$u_{\mathrm{C}} = \frac{(\dot{m}_{\mathrm{LE}}/\rho_{\mathrm{LE}}) + (\dot{m}_{\mathrm{GC}}/\rho_{\mathrm{GC}})}{(1 - ((2\delta)/d_{\mathrm{T}}))^2}. \tag{25}$$

The interfacial friction factor, f_{I}, is calculated through a correlation suggested by Hewitt and Whalley [15]

$$f_{\mathrm{I}} = f_{\mathrm{SC}}\left[1 + 24\left(\frac{\rho_{\mathrm{LF}}}{\rho_{\mathrm{G}}}\right)^{1/3}\frac{\delta}{d_{\mathrm{T}}}\right], \tag{26}$$

where f_{SC} is the friction factor for a single phase flow in a tube with the same diameter, density ρ_{C}, velocity u_{C} and viscosity equal to that of the gas phase.

The total pressure gradient is given by

$$\frac{\mathrm{d}p}{\mathrm{d}z} = \frac{\mathrm{d}p}{\mathrm{d}z_{\mathrm{a}}} + \frac{\mathrm{d}p}{\mathrm{d}z_{\mathrm{f}}} + \frac{\mathrm{d}p}{\mathrm{d}z_{\mathrm{g}}}. \tag{27}$$

In the gas core, a force balance over an element $\mathrm{d}z$ gives the following expressions for the components of the pressure gradient:

$$\frac{\mathrm{d}p}{\mathrm{d}z_{\mathrm{a}}} = -(u_{\mathrm{C}} - u_{\mathrm{LF}})\left[\frac{\mathrm{d}\dot{m}_{\mathrm{GC}}}{\mathrm{d}z} + \frac{4}{d_{\mathrm{T}}}(E + D)\right] - \frac{\mathrm{d}u_{\mathrm{C}}}{\mathrm{d}z}\left[\dot{m}_{\mathrm{GC}} + \dot{m}_{\mathrm{LE}}\right], \tag{28}$$

$$\frac{\mathrm{d}p}{\mathrm{d}z_{\mathrm{f}}} = -4\frac{\tau_{\mathrm{I}}}{(d_{\mathrm{T}} - 2\delta)}, \tag{29}$$

$$\frac{\mathrm{d}p}{\mathrm{d}z_{\mathrm{g}}} = -\rho_{\mathrm{C}} g, \tag{30}$$

where

$$\frac{\mathrm{d}u_{\mathrm{C}}}{\mathrm{d}z} = \frac{(\mathrm{d}\dot{m}_{\mathrm{LE}}/\mathrm{d}z)(1/\rho_{\mathrm{LE}}) + (\mathrm{d}\dot{m}_{\mathrm{GC}}/\mathrm{d}z)(1/\rho_{\mathrm{GC}})}{(1 - (2\delta/d_{\mathrm{T}}))^2}. \tag{31}$$

The accelerational pressure drop is composed of three terms: (i) the acceleration of droplets and vaporised gas from the liquid film velocity to the mean gas core velocity; (ii) the deceleration of droplets deposited on the annular film and (iii) the acceleration of mass in the gas core due to velocity changes.

In multicomponent evaporating systems, the difference in volatility between the components gives rise to axial gradients of concentration (and hence of saturation temperature) in both liquid and vapour streams due to the preferential evaporation of the more volatile component(s) even when local component equilibrium occurs. In annular flow, such an equilibrium situation is broken down by droplet entrainment and deposition since liquid is exchanged between different sections of the pipe. Moreover, the droplets themselves, at a given distance, will have a mean concentration different from that of the liquid film. A simplified approach to the phenomenon pursued in the present work suggests that, if the vaporisation rate of the liquid film is much higher than that of the droplets in the core, then it is not illogical to assume that, whilst in the vapour core, the droplets retain a concentration approximately equal to that of the liquid film at the point where they were created (entrained). Thus, droplets generated at distinct co-ordinates have distinct concentrations and, at a particular co-ordinate, a spectrum of concentration is found in the population of depositing droplets.

The following differential equations are obtained through mass balances over an element of tube of length $\mathrm{d}z$ (see Fig. 2). Eqs. (32)–(34) represent overall mass conservation for the liquid film, vapour core and liquid entrained as droplets. Eq. (35) is a component mass balance for the liquid film. The effect of deposition of droplets having different concentrations is characterised by the expression in parenthesis in the RHS of (35).

$$\frac{\mathrm{d}}{\mathrm{d}z}\dot{m}_{\mathrm{LF}} = \frac{4}{d_{\mathrm{T}}}\Big(\langle D\rangle - E - \dot{m}_{\mathrm{I}}\Big), \tag{32}$$

$$\frac{\mathrm{d}}{\mathrm{d}z}\dot{m}_{\mathrm{GC}} = \frac{4}{d_{\mathrm{T}}}\dot{m}_{\mathrm{I}}, \tag{33}$$

$$\frac{\mathrm{d}}{\mathrm{d}z}\dot{m}_{\mathrm{LE}} = \frac{4}{d_{\mathrm{T}}}(E - \langle D\rangle), \tag{34}$$

$$\frac{\mathrm{d}}{\mathrm{d}z}x_{\mathrm{LF,i}} = \frac{4}{d_{\mathrm{T}}\dot{m}_{\mathrm{LF}}}\Big[(\langle Dx_{\mathrm{LF,i}}\rangle - \langle D\rangle x_{\mathrm{LF,i}}) + \dot{m}_{\mathrm{I}}x_{\mathrm{LF,i}} - \dot{m}_{\mathrm{I,i}}\Big]. \tag{35}$$

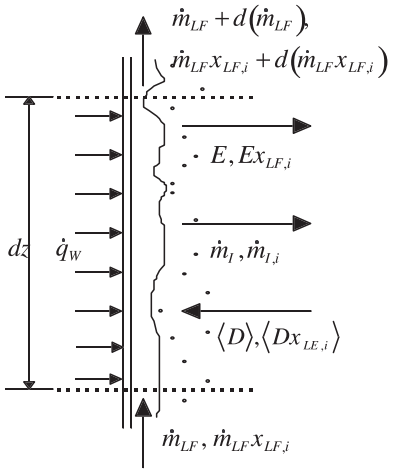

Fig. 2. Mass balance over an element of length dz.

$\dot{m}_{\mathrm{I,i}}$ is the mass flux of component i in the evaporating stream. The calculation of $\dot{m}_{\mathrm{I,i}}$ (and hence of $\dot{m}_{\mathrm{I}} = \sum_{i=1}^{2} \dot{m}_{\mathrm{I,i}}$) is carried out using a model for simultaneous heat and mass transfer, which is described in Part II of this paper. The modelling is based on a film (or Colburn) method in which the effect of droplet interchange is taken into account in the interfacial heat balance.

The balance equations are solved by a fifth order Runge–Kutta method [11]. At each marching step m of length dz, the values of $n_{\mathrm{D}}^{j,m}$ (and consequently of $D^{j,m}$, $\langle D^m\rangle$ and E^m) are calculated and used to compute the mass fluxes and total pressure drop. In an evaporating system in which single phase liquid is fed to the channel, annular flow will not occur until the vapour velocity is sufficient to satisfy Eq. (1). For sub-annular flow regimes occurring in the first part of the channel, the Friedel [16] correlation is used to compute the wall shear stress.

Published routines for calculating physical and thermodynamic properties of mixtures [17] were incorporated in the code. Densities, enthalpies and specific heat capacities were calculated through the method by Lee and Kesler [18], viscosities and thermal conductivities via the method by Ely and Hanley [19,20] and surface tension using the method by Sprow and Prausnitz [21].

A significant amount of liquid may be entrained as droplets at the onset of annular flow, perhaps as a result of high liquid entrainment also present in the churn flow regime [14]. There is at present no general method for calculating the entrained fraction at the onset of annular flow. One possible assumption is that deposition and entrainment are at equilibrium (i.e., equal) at this point; for the present analysis, this would give entrained fractions in the range 5–10% at the onset of annular flow. However, this takes no account of the proximity to churn flow and the actual values are likely to be higher. In the present work, the approach has been to assume a series of values covering the likely range (i.e., 0, 10, 20 and 40%) and to carry out calculations for each of these values.

The set of equations derived above enables one to calculate the mass fraction of droplets which, having been created at a section j, still are entrained in the core at a section m downstream

$$e^{j,m} = \frac{\dot{m}_{\mathrm{LE}}^{j,m}}{\langle \dot{m}_{\mathrm{LE}}^{m} \rangle}. \tag{36}$$

The mean concentration in the droplets in the core is given by

$$x_{\mathrm{LE,i}} = \frac{\langle \dot{m}_{\mathrm{LE}}^{m} x_{\mathrm{LE,i}}^{m} \rangle}{\langle \dot{m}_{\mathrm{LE}}^{m} \rangle}. \tag{37}$$

These quantities are of crucial importance to the analysis as they indicate the imbalance of concentration between the droplet core and the liquid film ($x_{\mathrm{LE,i}}$) and between groups of droplets ($e^{j,m}$). Again, such imbalances develop due to the preferential evaporation of the more volatile component(s).

3. Results

To assess the performance of the modelling work presented in both parts of this paper, comparisons are made with the experimental data obtained by Kandlbinder [2]. Kandlbinder carried out forced convective boiling experiments for both pure hydrocarbons (*n*-pentane, *n*-hexane and iso-octane) and their mixtures in a 8.68 m long, vertical 321 stainless steel tube test section. The inner and outer diameters were 25.4 and 38.0 mm, respectively. Along the test section, bulk fluid and wall temperatures were measured. Bulk temperatures (i.e., the temperatures of the fluid at the centre line of the tube) were measured at 12 equally spaced (750 mm) locations. Wall temperatures were measured at 74 points along the test section. Also, the pressure distribution was recorded by 12 pressure transducers distributed along the test section.

In the present work, results for two binary mixtures of *n*-pentane/iso-octane with overall mole fractions of 0.7/0.3 (mixture 1) and 0.35/0.65 (mixture 2) are analysed. The range of conditions covered in the simulations is shown in Table 1.

Figs. 3(a) and (b) show typical curves for the decay of initial droplet mass fraction, $e^{0,m}$, for Runs 1 and 3, respectively. $e^{0,m}$ is plotted against a modified axial co-ordinate, $z_{\mathrm{A}} = z - z_{\mathrm{OA}}$, z_{OA} being the co-ordinate at which the onset of annular flow takes place. In each graph, the value of total initial entrained fraction, defined as the mass flux of entrained liquid divided by the total mass flux of liquid (in the film and in the droplets),

Table 1
Summary of conditions in calculations

Run no.	$\tilde{x}_{ov}$	p (MPa)	$\dot{q}_W$ (kW m^{-2})	$\dot{m}_T$ (kg m^{-2} s^{-1})
Run 1	0.7/0.3	0.23	57.7	286.6
Run 2	0.7/0.3	0.30	59.6	303.1
Run 3	0.7/0.3	0.60	60.2	295.0
Run 4	0.7/0.3	0.23	49.8	292.8
Run 5	0.7/0.3	0.61	68.4	503.8
Run 6	0.7/0.3	0.32	49.3	305.0
Run 7	0.7/0.3	1.00	49.1	299.2
Run 8	0.35/0.65	0.22	59.4	295.2
Run 9	0.35/0.65	0.29	58.9	302.2
Run 10	0.35/0.65	0.61	59.1	304.9
Run 11	0.35/0.65	0.22	40.7	195.8
Run 12	0.35/0.65	0.22	49.3	297.1

is varied from 0% to 40%. It can be observed that higher the initial entrained fraction, the lower the rate of decay of $e^{0,m}$, suggesting that the mean concentration of the entrained droplets is affected by the variation of initial entrained fraction.

Table 2 compares the values of $e^{0,m}$ for both mixtures under similar conditions using different initial entrained fractions. As the portion of the pipe over which annular flow occurs is different for each condition (basically due to distinct sub-cooling temperature differences at the pipe inlet), $e^{0,m}$ values are compared at a co-ordinate 1 m downstream to the point of onset of annular flow, z_{OA}.

The data in Table 2 reveal that $e^{0,m}$ increases with pressure and is comparatively higher for mixture 2 (richer in the less volatile component). In addition, the rate of increase of $e^{0,m}$ with pressure is also higher for mixture 2. A possible explanation for these trends may be due to a change in the physical properties of the mixture with both pressure and overall composition. This would, in turn, be reflected on a variation of entrainment and deposition rates.

Typical profiles of bulk concentration (mass fraction) of *n*-pentane for the film and for the droplets are shown in Figs. 4(a) and (b). In each graph, the initial amount of liquid entrained as droplets is again varied from 0% to 40%. This alteration provokes an opposite effect in the behaviour of concentration in both streams; higher values of initial $\dot{m}_{LE}$ induce lower profiles of $x_{LF,1}$ and higher profiles of $x_{LE,1}$.

Figs. 5(a) and (b) show comparisons between experimental data and predictions of absolute pressure distributions. As expected [22], the influence of the initial liquid entrained fraction on the pressure gradient is not as pronounced as on the profiles of liquid concentration. The average deviation in the absolute pressure predictions at high qualities lies within the 10–15% range.

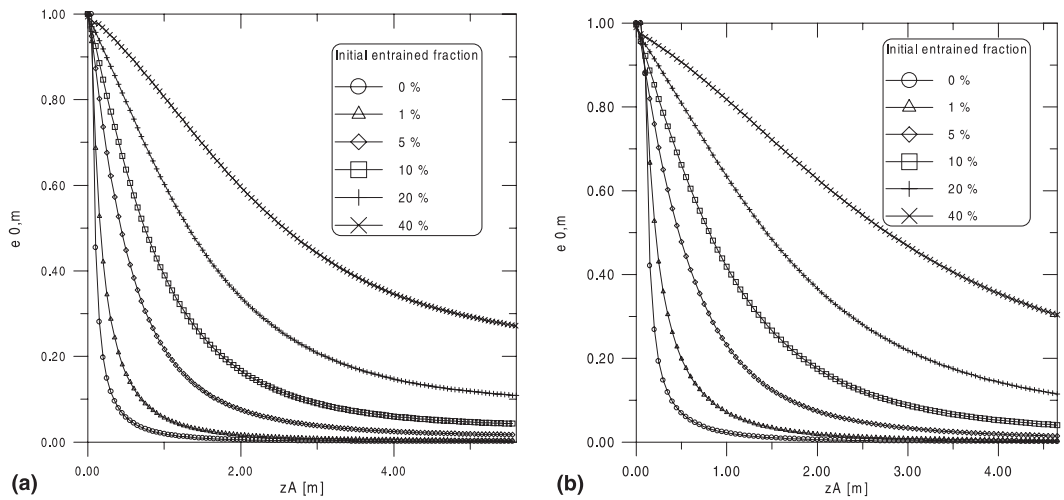

Fig. 3. Typical curves of $e^{0,m}$ for different initial entrained fractions: (a) Run 1; (b) Run 3. Conditions are those of Table 1.

Table 2
Values of $e^{0,m}$, at $z_A = 1$ m, for different values of initial entrained fraction

Mixture 1					Mixture 2				
Run no.	0%	10%	20%	40%	Run no.	0%	10%	20%	40%
Run 1	0.019	0.389	0.602	0.797	Run 8	0.019	0.396	0.607	0.800
Run 2	0.019	0.398	0.611	0.804	Run 9	0.022	0.407	0.621	0.810
Run 3	0.022	0.418	0.634	0.818	Run 10	0.023	0.430	0.642	0.822

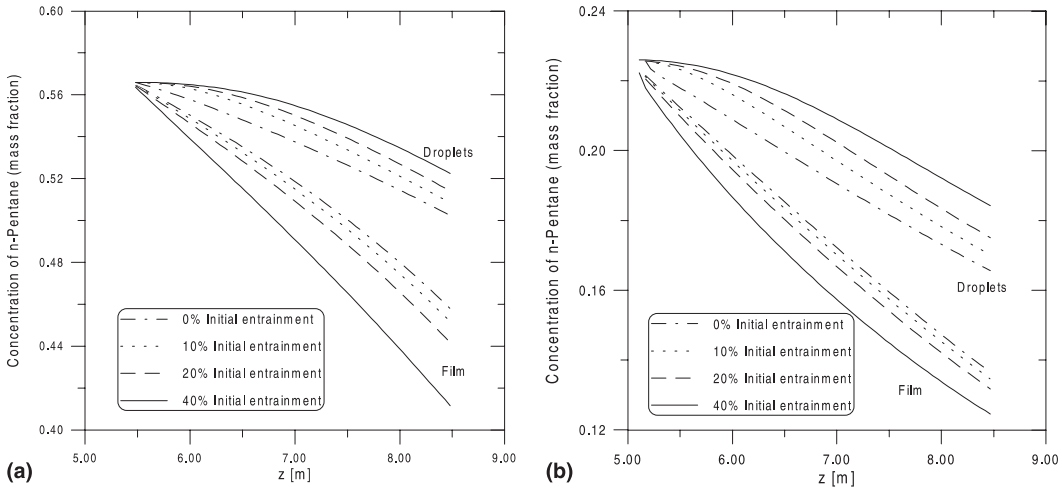

Fig. 4. Mean concentration of *n*-pentane in the liquid film and in the droplets: (a) Run 5; (b) Run 12. Conditions are those of Table 1.

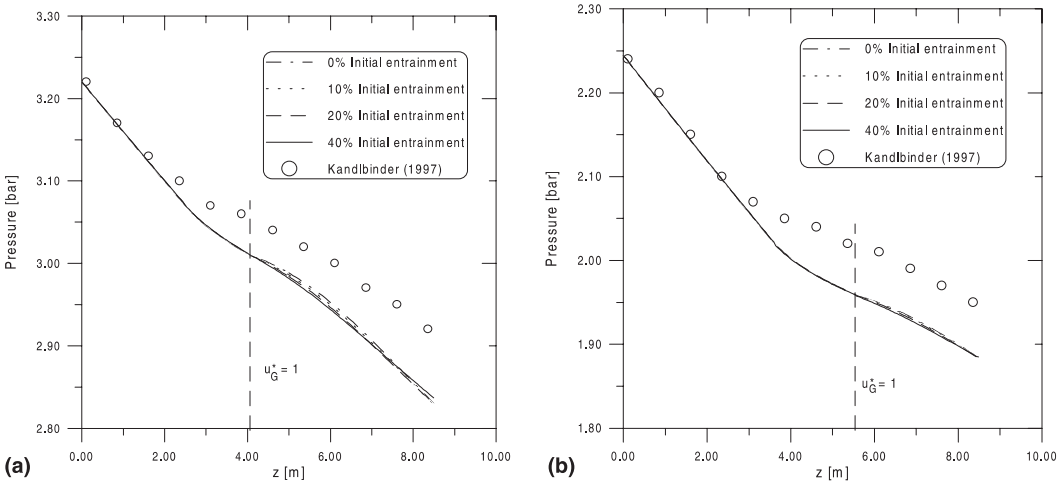

Fig. 5. Profiles of absolute pressure: (a) Run 6; (b) Run 11. Conditions are those of Table 1.

However, it can be observed that the predicted gradients of pressure in the annular flow region are in very good agreement with those observed from the experimental data. This leads to the conclusion that the discrepancies in the absolute pressure values at high qualities are due to a poor prediction of pressure gradients at moderate qualities (mainly churn flow regime). A detailed understanding of the physics of such flows is not yet fully

achieved and the need for more physically based models (especially for churn flow) is evident.

4. Conclusion

An investigation of the interchange of mass between the film and the droplet core in annular flow of evaporating binary mixtures was presented. A droplet interchange model based on the set of correlations by Govan et al. [1] for pure fluids was proposed and embedded into an annular flow modelling framework so that relevant flow parameters could be calculated and analysed. The main conclusions arising from this analysis are as follows:

1. In the annular flow regime, the mechanism of droplet entrainment and deposition coupled with the preferential evaporation of the more volatile component from the liquid film causes the local concentration in the liquid film to be different from that in the entrained droplets. Axial gradients of mean concentration occur in both liquid streams.
2. The definition of the parameter $e^{0,m}$, i.e., the mass fraction of droplets which, being created at the point of onset of annular flow, are still entrained in the core at a section m downstream, allows one to assess the influence of the amount of liquid initially entrained as droplets on the liquid concentration profiles.
3. Higher axial profiles of mean concentration of the more volatile component, and hence lower profiles of mean temperature, were observed for the droplet in core as the entrained fraction at the onset of annular flow was increased. An opposite trend was observed for the liquid film, as less liquid was available in the film for evaporation.

The effects of mass transfer resistance, the calculation of interfacial parameters (mass fluxes, compositions and temperature) and heat transfer predictions are described in detail in the second part of this paper.

Acknowledgements

The first author thanks the Brazilian National Research Council (CNPq - Conselho Nacional de Desenvolvimento Científico e Tecnológico) for the award of a scholarship (Grant No. 200085/97-2).

References

[1] A.H. Govan, G.F. Hewitt, D.G. Owen, T.R. Bott, An improved CHF modelling code, in: Proceedings of the Second UK National Heat Transfer Conference, Institution of Mechanical Engineers, London, UK, 1988, pp. 33–48.

[2] T. Kandlbinder, Experimental investigation of forced convective boiling of hydrocarbons and hydrocarbon mixtures, Ph.D. thesis, University of London, Imperial College, 1997.

[3] T. Kandlbinder, V.V. Wadekar, G.F. Hewitt, Mixture effects for flow boiling of a binary hydrocarbon mixture, in: J.S. Lee (Ed.), Proceedings of the 11th International Heat Transfer Conference, Taylor and Francis, Philadelphia, PA, 1998, pp. 303–308.

[4] P. Hutchinson, P.B. Whalley, A possible characterisation of entrainment in annular flow, Chem. Eng. Sci. 28 (1973) 974–975.

[5] S.A. Schadel, G.W. Leman, J.L. Binder, T.J. Hanratty, Rates of atomisation and deposition in vertical annular flow, Int. J. Multiphase Flow 16 (1990) 363–374.

[6] V.I. Milashenko, B.I. Nigmatulin, V.V. Petukhov, N.I. Trubkin, Burnout and distribution of liquid in evaporative channels of various lengths, Int. J. Multiphase Flow 15 (1989) 393–401.

[7] P.B. Whalley, B.J. Azzopardi, G.F. Hewitt, R.G. Owen, A physical model for two-phase flows with thermodynamic and hydrodynamic non-equilibrium, in: U. Grigull (Ed.), Proceedings of the Seventh International Heat Transfer Conference, vol. 5, Hemisphere, New York, 1982, pp. 181–188.

[8] G.B. Wallis, One Dimensional Two-phase Flow, McGraw-Hill, New York, 1969.

[9] A.W Bennett, G.F. Hewitt, H.A. Kearsey, R.K.F. Keeys, Heat transfer to steam-water mixtures flowing in uniformly heated tubes in which the critical heat flux has been exceeded, Thermodynamics and Fluid Mechanics Convention, Institution of Mechanical Engineers, Bristol, UK, 1967, Paper 27.

[10] B.J. Azzopardi, G. Freeman, D.J. King, Drop sizes and deposition in annular two-phase flow, UKAEA Report AERE-R9634, 1980.

[11] W.H. Press, S.A. Teukolsky, W.T. Vetterling, B.P. Flannery, Numerical Recipes in FORTRAN – The Art of Scientific Computing, second ed., Cambridge University Press, New York, 1992.

[12] N. Hawkes, Wispy-annular flow, Ph.D. thesis, University of London, Imperial College, 1996.

[13] G.F. Hewitt, Analysis of annular two-phase flow; application of the Dukler analysis to vertical upward flow in a tube, UKAEA Report AERE-3680, 1961.

[14] G.F. Hewitt, N.S. Hall-Taylor, Annular Two-phase Flow, Pergamon Press, London, 1970.

[15] G.F. Hewitt, P.B. Whalley, The correlation of liquid entrained fraction and entrainment rate in annular two-phase flow, UKAEA Report AERE-9187, 1978.

[16] L. Friedel, Improved friction pressure drop correlations for horizontal and vertical two-phase pipe flow, 27th European Two-Phase Flow Group Meeting, Ispra, Italy, 1979, Paper E2.

[17] M.J. Assael, J.P.M. Trusler, T.F. Tsolakis, Thermophysical Properties of Fluids, Imperial College Press, London, 1996.

[18] B.I. Lee, M.G. Kesler, A generalized thermodynamic correlation based on three-parameter corresponding states, AIChE J. 21 (1975) 510–527.

[19] J.F. Ely, H.J.M. Hanley, Prediction of transport properties. 1. Viscosities of fluids and mixtures, Ind. Eng. Chem. Fundam. 20 (1981) 323–332.

[20] J.F. Ely, H.J.M. Hanley, Prediction of transport properties. 2. Thermal conductivity of pure fluids and mixtures, Ind. Eng. Chem. Fundam. 22 (1983) 90–97.
[21] F.B. Sprow, J.M. Prausnitz, Surface thermodynamics of liquid mixtures, Can. J. Chem. Eng. 45 (1967) 25–28.
[22] A.H. Govan, Modelling of vertical annular and dispersed two-phase flows, Ph.D. thesis, University of London, Imperial College, 1990.